Silver Anchored α-MnO_2 Nanorods Based SERS Substrates for Salivary Thiocyanate Detection and Application in Oral Cancer Diagnosis

Navami Sunil, Rajesh Unnathpadi, and Biji Pullithadathil*
Nanosensor Laboratory, PSG institute of Advanced Studies, Coimbatore 641004, India

***e-mail:** pbm@psgias.ac.in

Abstract. Salivary sensors are ideal non-invasive diagnostic platforms for cancer detection owing to the existence of many proteins and metabolites that can reflect individual's health status. Elevated levels of thiocyanate (SCN^-) in smokers' saliva may be a potential biomarker indicating increased oral cancer risk due to the nitrosation process. Herein, we report a highly sensitive, label-free, ultrasensitive surface-enhanced Raman spectroscopy (SERS) detection of salivary thiocyanate using silver anchored α-MnO_2 nanorods based SERS substrates for the early detection of oral cancer. The structural and morphological characterization of the synthesised Ag/ α-MnO_2 nanorods have been performed using XRD, FTIR, and TEM analysis. The intensity of SERS peak at around 2170 cm^{-1}, originating from the −C≡N stretching mode, indicated the concentrations of SCN^- ions. The SERS spectra of SCN^- was recorded at concentrations ranging from 1 to 6 mM, which was utilised to differentiate between smokers and non-smokers and hence to predict the risk of oral cancer. © 2023 Journal of Biomedical Photonics & Engineering.

Keywords: salivary sensors; non-invasive diagnosis; oral cancer; surface enhanced Raman spectroscopy; thiocyanate.

Paper #7203 received 21 Feb 2023; revised manuscript received 19 Apr 2023; accepted for publication 24 Jun 2023; published online 31 Aug 2023. doi: 10.18287/JBPE23.09.030311.

1 Introduction

Oral and oropharyngeal cancers are a diverse group of tumours that originate in the buccal mucosa, hard and soft palate, tongue, and oropharyngeal sub-sites such as the tonsils, posterior pharyngeal wall and tongue base. Oral cancer is the world's sixth most common cancer and is a major concern in Southeast Asia, owing to the prevalence of oral habits such as betel quid chewing, smoking, and alcohol consumption [1]. Tobacco use is linked to a variety of changes in the oral mucous membrane, ranging from benign and reversible lesions such as smoker's mouth to cancerous lesions from the palate to oral cancer. Saliva-based tests have several advantages, including ease of use, cost savings, non-invasiveness, and the ability to repeat sampling.

Thiocyanate (SCN) is a naturally occurring component of bodily fluids such as serum, saliva, urine, and tears which enters the human body through the consumption of Brassica vegetables, milk, and cheese. Thiocyanate, a significant cyanide metabolic by-product, is a key indicator of smoke inhalation along with carbon monoxide, nicotine, and cotinine. Its main sources in the human body are diet and tobacco and is secreted in saliva and has a half-life of 10−14 days [2]. Tobacco is known to suppress the immune system and is a well-known cause of adult periodontitis, leukoplakia and oral submucous fibrosis which have the potential for malignant transformation [3]. It is clear that smoking and oral cancer have a clear dose-response relationship. In normal non-smokers, salivary SCN^- concentrations range from 0.5 to 2 mM, with an average of 1 mM. Heavy smokers, on the other hand, may have salivary concentrations as high as 6 mM [4]. This elevated level of SCN in smokers' saliva may be responsible for the increased cancer risk of smokers due to the nitrosation process [5].

Although non-invasive quantitative assessment of the chemical compositions of saliva are possible through many methods such as ELISA, micro-satellite analysis,

This paper was presented at the International Conference on Nanoscience and Photonics for Medical Applications – ICNPMA, Manipal, India, December 28–30, 2022.

and high performance liquid chromatography (HPLC), mass spectrometry (MS) and can potentially detect these bio molecular changes, these highly specific techniques in molecular detection are typically labour-intensive procedures that require long analysis time. Raman spectroscopy-based spectral analysis of bio-fluids for disease diagnosis and screening may represent a potentially viable avenue for cancer diagnosis and is emerging as a potentially useful clinical adjunct, capable of identifying and differentiating the subtle changes in tissue biochemistry associated with oral disease and cancer progression in a label-free and non-invasive manner [6]. Recently, semiconductor nanostructures have been discovered to have the potential to improve SERS. Many studies have shown that synthesised semiconductor-noble metal nanocomposites have significant Raman enhancement effects [7]. Manganese oxide (MnO_2) has been extensively studied as a common metal oxide due to its low cost, natural abundance, diverse morphologies, and low toxicity. These advantages allow it to be used in a variety of applications such as catalysis, ion exchange, molecular adsorption, biosensors, and energy storage. MnO_2 can be formed into particles, rods, wires, tubes, sheets, and 3D porous nanostructures, with porous MnO_2 frameworks being a significant research area due to their superiority to bulk counterparts in many aspects.

In this investigation, we report a simple method for fabricating α-MnO_2 nanorods using hydrothermal method, followed by functionalization with Ag nanoparticles (AgNPs) using wet chemical method. α-MnO_2 nanorods can provide both smooth surfaces for homogeneous silver aggregation and sharp edges for the formation of hot spots. Because of the generation of homogeneous multiple hot spots and the propagation of SPRs, reliable and stable SERS signals can be expected after the arrangement of silver NPs on nanorods. The developed Ag@MnO_2 based SERS substrates are used for the detection of thiocyanate further extending its application to oral cancer diagnosis.

2 Experimental Details

2.1 Materials and Methods

Pottassium permanganate ($KMnO_4$, 99.5%, SRL) Polyvinyl pyrrolidone (PVP, average molecular weight = 360,000), Nitric acid (HNO_3, Merck), Silver Nitrate ($AgNO_3$, Merck), Sodium borohydride ($NaBH_4$, Merck), Ethylene glycol (EG, Merck), Pottassium thiocyanate (Isotherm) were used for the synthesis of Ag/α-MnO_2 NRs. All reagents were of analytical grade and directly used without any further purification.

2.2 Synthesis of α-MnO_2 Nanorods

α-MnO_2 nanorods were synthesised using the hydrothermal method [8–10] as described below. 6.7 g of $KMnO_4$ was first dissolved in 50 mL of de-ionized water and the mixture was stirred for 10 min. Following that, 4.2 mL of HNO_3 was dropped into the desired mixture and vigorously stirred for an hour. The resulting mixture was then transferred to a 50 mL Teflon-lined stainless-steel autoclave and kept at 120 °C in the furnace for 12 h. Following the reaction, the obtained brown product was washed several times with DI water and centrifuged. Finally, the as-synthesized product was dried overnight in an oven at a constant temperature of 80 °C before being characterised. For the synthesis of silver decorated α-MnO_2 NRs, 100 mL of ethylene glycol was treated with 400 mg of α-MnO_2 nanowires and 130 mg of PVP (polyvinyl pyrrolidone).

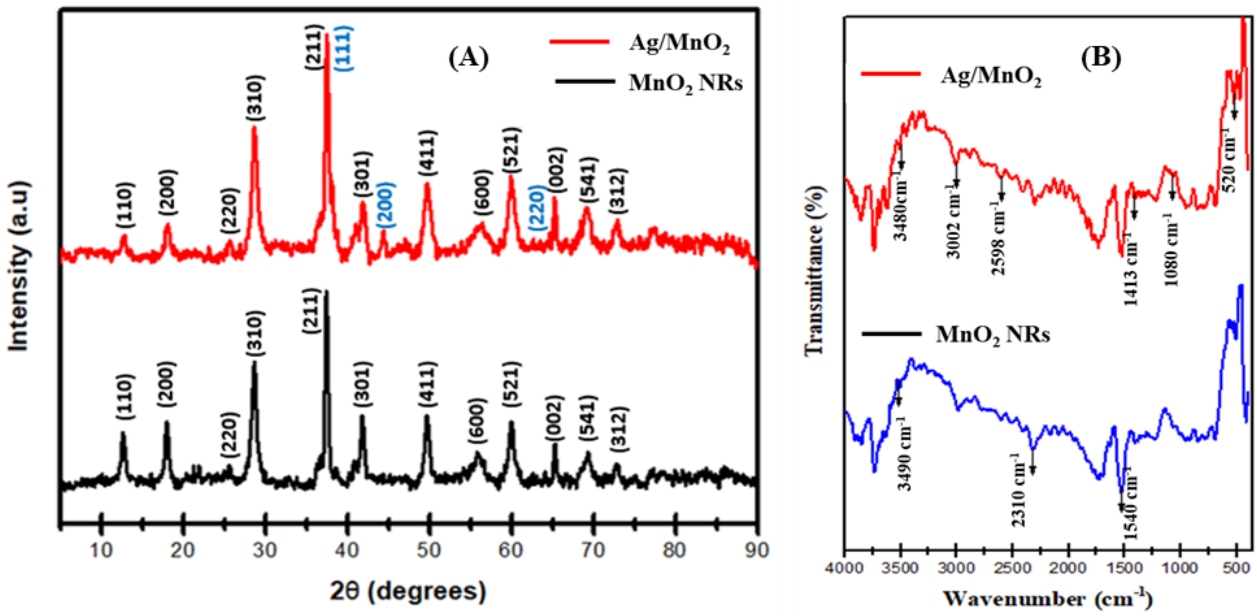

Fig. 1 (A) XRD patterns and (B) FTIR spectra of α-MnO_2 NRs and Ag anchored α-MnO_2 NRs.

The suspension was transferred to a 250 mL round-bottom flask and vigorously stirred at 90 °C for 20 min. The reaction flask was then filled with $NaBH_4$ (1.0 mmol) and 2 mL of 0.1 M $AgNO_3$ solutions. This mixture was stirred for another 12 h to produce Ag@MnO_2, which was washed three times with ethanol and water followed by successive rounds of centrifugation supernatant removal. Finally, the product was vacuum dried.

2.3 Saliva Sample Collection

Human saliva (female, 20–30 years) was collected between 9:00 am to 10:00 am to avoid the interference from the food. Prior to the sample collection, the mouth was washed thrice with pure water. A non-stimulated collecting procedure was used in which the saliva was spit directly into a disposable cup. The sample was then transferred to a 2 mL centrifuge tube and centrifuged at 12,000 rpm for 15 min at 4 °C to remove the oral mucous epithelium cells and food debris and stored at 4 °C until analysis.

Different concentrations of the thiocyanate ranging from 1 mM to 6 mM were prepared. Then, 0.5 mL of the saliva was mixed with 0.5 mL of different concentrations of the thiocyanate solutions and 5 uL of the as prepared spiked sample is drop cased on the surface of the SERS substrate, dried and analysed.

2.4 Preparation of SERS Substrate

The glass slides were thoroughly cleaned with ethanol and ultrasonic oscillation for 30 min. After drying, the synthesized Ag@MnO_2 was drop-casted on cleaned glass slides and dried to produce the SERS substrate. Different concentrations of thiocyanate were prepared. The known concentration of thiocyanate solution was dropped on the surface of the prepared SERS substrate, dried before SERS measurements for SCN^- detection. Finally, SERS signals were collected at random locations. To evaluate the ability of Ag@MnO_2 NRs to detect SCN^- in the human saliva, the saliva sample was spiked with different concentrations of the thiocyanate ranging from 1 mM to 6 mM. 20 uL of the saliva containing spiked SCN^- was then dropped on the developed Ag@MnO_2 based SERS substrates and dried prior to SERS analysis.

2.5 Characterization Techniques

The structural and morphological characterization of Ag@MnO_2 NRs was carried out using transmission electron microscopy (JEM-2010, 200 kV, JEOL, Japan) integrated with EDAX. X-ray diffraction (XRD) measurements were acquired using a PANalytical X-pert diffractometer (Malvern) with Cu Kα radiation (λ = 1.54 Å) as the source. SERS spectra was acquired using confocal Raman microscope (WITec alpha300 RA, Ulm, Germany) equipped with 532 nm laser.

3 Results and Discussion

3.1 Characterization of Ag@MnO_2 NRs

The silver decorated α-MnO_2 Nano rods (Ag@MnO_2 NRs) were synthesized by a simple hydrothermal method and were characterized through, X-ray powder diffraction (XRD), Fourier transform infrared spectroscopy (FTIR), and transmission electron microscopy (TEM) analysis. The XRD pattern of α-MnO_2 NRs and Ag@MnO_2 NRs is depicted in Fig. 1A, indicating a number of distinct sharp diffraction peaks. The diffraction peaks in the XRD spectrum at 18.10°, 25.71°, 28.84°, 36.69°, 37.52°, 39.01°, 41.96°, 49.86°, 56.37°, 60.27°, 65.10°, and 69.71° are assigned to the planes (200), (220), (310), (400), (211), (330), (301), (411), (600), (521), (002) The XRD spectrum clearly shows high crystallinity and directional growth of α-MnO_2 NRs (221). In the XRD pattern, no contaminants or residues are detected, demonstrating the high purity of as-synthesized α-MnO_2 NRs.

The XRD pattern of Ag@MnO_2 revealed the presence of α-MnO_2 and metallic silver, with diffraction peaks at 38.12°, 44.28°, and 64.43° assigned to the crystal faces (111), (200), and (220) of silver indicating that silver nanoparticles had been successfully supported on the α-MnO_2 nanorods. Fig. 1B shows the FTIR spectra of as-synthesized MnO_2 and Ag@MnO_2. It can be seen that the FTIR spectrum of the α-MnO_2 showed very weak absorptions at 2310 cm^{-1}, and 1540 cm^{-1}, which correspond to the stretching and bending vibrations of water molecules or hydroxyl groups because the nano crystalline materials exhibit a high surface-to volume ratio. Peaks at 1080 cm^{-1} and 520 cm^{-1} correspond to the typical Mn-O stretching, bending, and wagging vibrations. The FTIR spectra of Ag@MnO_2 exhibits various peaks at 2598 cm^{-1}, 1413 cm^{-1}, and CH_2 in plane bending, respectively.

The morphologies and structural characteristics of the Ag@MnO_2 nanorods could be observed diametrically by TEM analysis. A typical TEM image of α-MnO_2 NRs shown in Fig. 2A evidently confirms nanorod-type surface morphology. The individual nanorods are clearly distinguishable. The clear lattice fringes illustrate that the nanorod is a single-crystal, and the interlayer space is about 0.7 nm, corresponding to the [110] plane of α-MnO_2.

TEM images in Fig. 2B reveal that silver nanoparticles are supported on α-MnO_2 nanorods. As shown in Fig. 2B, it is clearly observed that the surface of the MnO_2 nanorods is coated with many small silver particles. The full-range EDS spectra of α-MnO_2 NRs and Ag@ α-MnO_2 NRs are shown in Fig. 2. Four elements (C, Ag, Mn, and O) were identified from the full-survey-scan spectrum of the Ag@MnO_2 composite. The peak of Cu was caused by the Cu micro grid on which the product was placed.

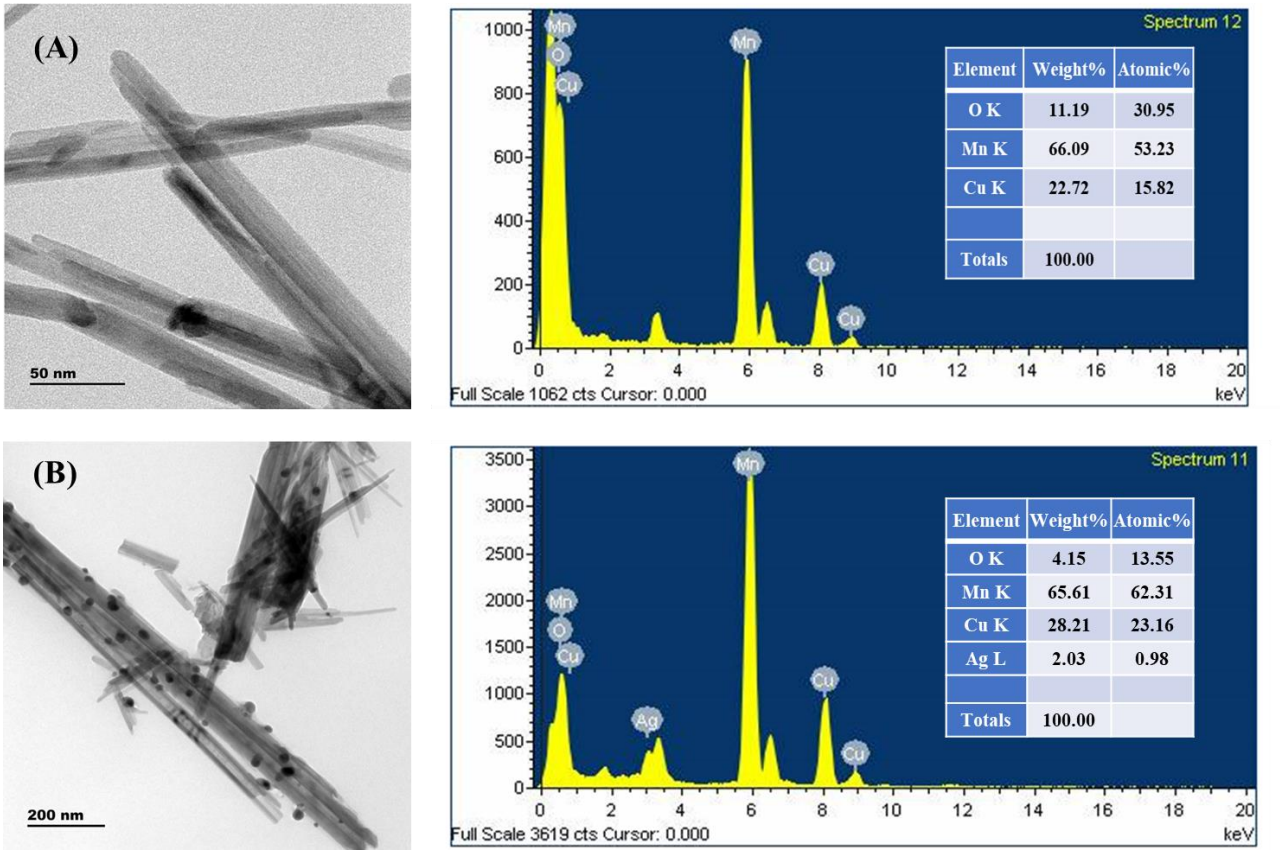

Fig. 2 TEM analysis and the corresponding EDS spectra of (A) α-MnO_2 NRs and (B) Ag@α-MnO_2 NRs.

3.2 SERS Detection of Thiocyanate

The feasibility of using the newly developed SERS substrate (Ag@MnO_2) to detect thiocyanate was investigated. SERS spectra was acquired using confocal Raman microscope (WITec alpha300 RA, Ulm, Germany) equipped with 532 nm laser. Both the material and the target analyte are active in this laser wavelength and 532 nm wavelength option is a workhorse for inorganic materials, offering maximum signal for samples that do not suffer from autofluorescence. Also, 532 nm is useful for Raman resonance experiments and for the study of metal oxide based materials. The excellent power stability, very low rms noise and perfect beam quality will meet all the requirements of most applications.

Copper (I) Thiocyanate (CuSCN) was used as the precursor for the preparation of different thiocyanate concentrations. A concentration of 1 M was used for the Raman spectra whereas 50 mM concentration was used for SERS. Fig. 3A shows the Raman spectrum of CuSCN in the regions of 20 cm^{-1} to 3500 cm^{-1}. There are four Raman peaks centred at 235 cm^{-1}, 420 cm^{-1}, 735 cm^{-1} and 2170 cm^{-1}, indicating CuSCN, which were well matched with the previous reports [11, 12]. The absorption peak at 753 cm^{-1} is caused by the C−S bond stretching vibration and the peak at 2170 cm^{-1} is attributed to the asymmetric stretching vibration of −C≡N bond, which is chosen as the characteristic peak for identifying of SCN^- due to its high intensity. The highest Raman peak at 2170 cm^{-1} showed an intensity enhancement of around 12,000 counts in the SERS spectra.

The physicochemical properties of plasmonically active nanoparticles are important parameters to consider when preparing nanostructures to produce substrates with a high SERS effect [13, 14]. The Raman intensity was found to be greatly enhanced when the Ag decorated α-MnO_2 nanorod was used as an efficient SERS substrate for the detection of thiocyanate (Fig. 3A). This massive enhancement is due to the strong localization of near field intensity, which results in the formation of so-called hot spots where the Raman signal from analyte molecules can be amplified orders of magnitude [15]. The greater enhancement of Ag@MnO_2 is explained by the higher concentration of Ag causing a more pronounced Plasmon excitation effect, which results in more efficient excitation of the Raman modes.

The enhancement factor can be calculated using the following Eq.:

$$Enhancement\ Factor(EF) = \frac{I_{SERS} \times C_{Raman}}{I_{Raman} \times C_{SERS}}, \quad (1)$$

where I_{SERS} = 11,642 a.u., C_{Raman} = 1 M, I_{Raman} = 1345 a.u., C_{SERS} = 50 mM, $EF = 11{,}642 \times 1/1345 \times 50 \times 10^{-3} = 0.17 \times 10^3$.

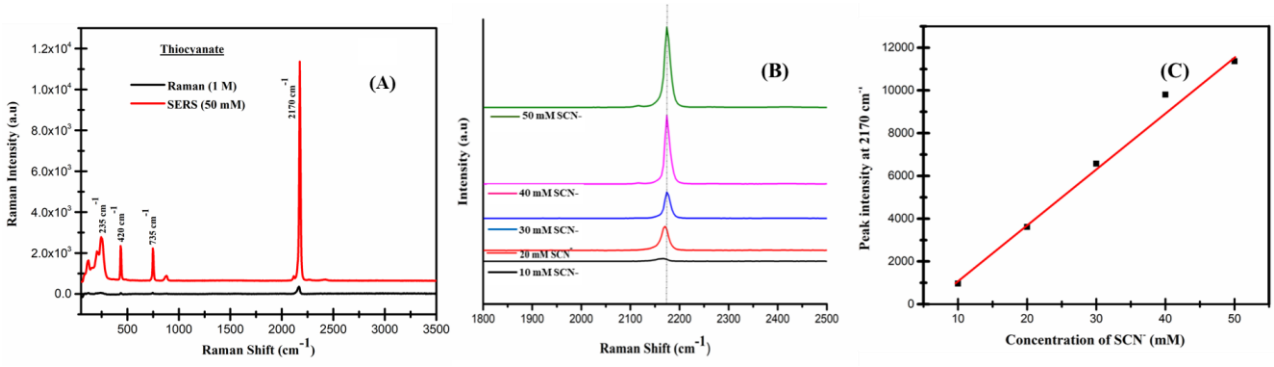

Fig. 3 Comparison of (A) Raman spectra of SCN^- and SERS spectra of SCN^- with Ag@MnO_2 as SERS substrate and (B) SERS spectra of different concentration of SCN^- (10 mM to 50 mM) and (C) the plot of peak intensity at 2170 cm^{-1} as a function of SCN^- concentration.

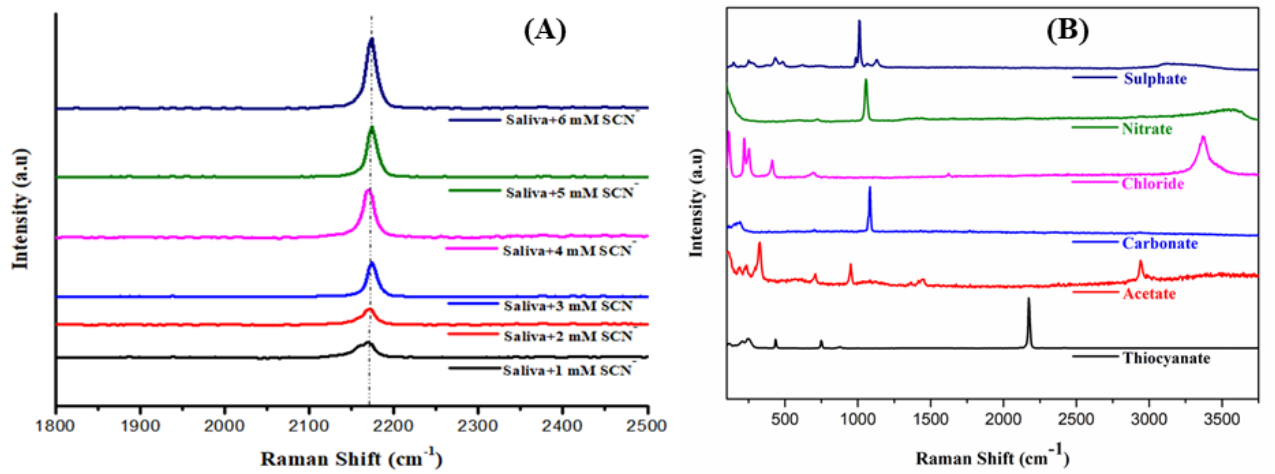

Fig. 4 (A) SERS spectra of saliva spiked with different concentrations of SCN^- (1 mM−6 mM) in Ag@MnO_2 SERS substrate and (B) the effect of interferents.

To assess the general applicability of Ag@MnO_2 for potential applications in bio-analytics, it was then used to detect thiocyanate (SCN^-) concentrations ranging from 10 mM to 50 mM as shown in the Fig. 3B. The SERS spectra showed increase in intensity with increase in the concentration of thiocyanate and the plot of peak intensity at 2170 cm^{-1} as a function of thiocyanate concentration was also found to be linear which is compatible with the existing literatures (Fig. 3C).

When SCN^- is added, a strong Raman band at 2170 cm^{-1} was appeared, which is attributed to the −CN stretching vibration mode. The results show that Ag@MnO_2 NRs can amplify the SCN^- Raman signal, and the SERS intensity at 2170 cm^{-1} can be used to detect the presence of SCN. To evaluate the ability of Ag@MnO_2 NRs to detect SCN^- in the human saliva, the saliva samples were spiked with different concentrations of the thiocyanate ranging from 1 mM to 6 mM. A SERS peak appears at around 2170 cm^{-1}, corresponding to the −C≡N stretching mode, which can be used to indicate the existence of SCN^- in human saliva [16−18]. By using the peak intensity at 2170 cm^{-1} to characterize the SERS signal, there exhibits a positive correlation between SERS intensity and ion concentration.

The SERS spectra of SCN^- with concentrations ranging from 1 mM to 6 mM are shown in Fig. 4A. The SERS intensity (2170 cm^{-1}) increased as expected with increasing thiocyante concentration, which is consistent with previous reports [19−22]. The developed substrate exhibited extremely high SERS activity and sensitivity, as well as exceptional signal stability and reproducibility, and can thus be used to distinguish between smokers and non-smokers and hence the risk of oral cancer.

The SERS sensor to detect SCN^- would be highly specific, because the Raman bands of most common chemical bonds are usually within the range of 500–2000 cm^{-1}, which is far away from the peak responsible for the –C≡N stretching mode (2170 cm^{-1}). As a proof of concept, the anions which shows the effect of interferents of other anions with the thiocyanate were studied. Acetate, carbonate, chloride, nitrate, and sulphate were the common anions interfering with the salivary thiocyanate. Thus, to study the effect of interferents, Ag@MnO_2 NRs were mixed with solutions containing 100 μM of different anion ions, including CH_3COOH^-, Cl^-, CO_3^{2-}, NO^{3-}, and SO_4^{2-}. The results shown in Fig. 4B indicate that the presence of these anions has little impact on the peak intensity at

2170 cm^{-1}. As a result, this peak can be confidentially used to indicate the concentration of SCN^- with high specificity.

4 Conclusion

Herein, we present a simple method for fabricating α-MnO_2 nanorods using a hydrothermal method, and then decorating these nanorod structures with Ag nanoparticles (AgNPs) using a wet chemical method. The feasibility of using the newly developed SERS substrate (Ag@MnO_2) to detect thiocyanate was investigated using the developed SERS substrate. The results show that Ag@MnO_2 NRs can amplify the SCN^- Raman signal, and the SERS intensity at 2170 cm^{-1} can be used to detect the presence of SCN. The SERS spectra of SCN^- with concentrations ranging from 1 to 6 mM was detected which is used to distinguish between the smokers and non-smokers and hence to predict the risk of oral cancer. This work could be further extended to real time saliva sample analysis for the detection of thiocyanate using the developed Ag@MnO_2 based SERS substrates, further extending its application to oral cancer diagnosis.

Acknowledgement

Authors wish to acknowledge DST-INSPIRE (DST/INSPIRE Fellowship/2020/IF200094) for the financial support. The authors also acknowledge the facilities and support provided by the management, PSG Sons and Charities, Coimbatore.

Ethical Approval

All procedures performed in this study were in accordance with the ethical standards. Ethical clearance was obtained from Institutional Human Ethics Committee, PSG Institute of Medical Science and Research, Coimbatore (Ref No: PSG/IHEC/2023Appr/FB/014) dated 23-02-2023 for the collection of human saliva samples.

Disclosures

The authors declare no conflict of interest.

References

1. M. Kumar, R. Nanavati, T. G. Modi, and C. Dobariya, "Oral cancer: Etiology and risk factors: A review," Journal of Cancer Research and Therapeutics 12(2), 458–463 (2016).
2. M. T. Ashby, A. C. Carlson, and M. J. Scott, "Redox buffering of hypochlorous acid by thiocyanate in physiologic fluids," Journal of the American Chemical Society 126(49), 15976–15977 (2004).
3. A. Madiyal, V. Ajila, S. G. Babu, S. Hegde, S. Kumari, M. Madi, S. Achalli, P. Alva, and H. Ullal, "Status of thiocyanate levels in the serum and saliva of non-smokers, ex-smokers and smokers," African Health Sciences 18(3), 727–736 (2018).
4. R. B. Silwal, B. Ojha, D. Bajracharya, and G. Silwal, "Correlation of Salivary Thiocyanate levels and Oral Cytological Changes in Smokers," Journal of College of Medical Sciences-Nepal 16(4), 259–266 (2020).
5. K. Tsuge, M. Kataoka, and Y. Seto, "Cyanide and thiocyanate levels in blood and saliva of healthy adult volunteers," Journal of Health Science 46(5), 343–350 (2000).
6. K. Guze, H. C. Pawluk, M. Short, H. Zeng, J. Lorch, C. Norris, and S. Sonis, "Pilot study: Raman spectroscopy in differentiating premalignant and malignant oral lesions from normal mucosa and benign lesions in humans," Head & Neck 37(4), 511–517 (2015).
7. A. Musumeci, D. Gosztola, T. Schiller, N. M. Dimitrijevic, V. Mujica, D. Martin, and T. Rajh, "SERS of semiconducting nanoparticles (TiO2 hybrid composites)," Journal of the American Chemical Society 131(17), 6040–6041 (2009).
8. X. Liu, L. Shi, W. Jiang, J. Zhang, and L. Huang, "Taking full advantage of KMnO4 in simplified Hummers method: A green and one pot process for the fabrication of alpha MnO2 nanorods on graphene oxide," Chemical Engineering Science 192, 414–421 (2018).
9. X. Zhao-Hui, L. Zhao-Lin, M. Fang-Wei, S. Li-Ping, H. Li-Hua, and Z. Hui, "Hydrothermal Synthesis of alpha-MnO2 Nanorods and Their Electrochemical Performances," Chinese Journal of Inorganic Chemistry 28(4), 691–697 (2012).
10. H. Luo, Y. Yang, B. Yang, Z. Xu, and D. Wang, "Silver/manganese dioxide nanorod catalyzed hydrogen-borrowing reactions and tert-butyl ester synthesis," Journal of Chemical Research 45(7-8), 708–715 (2021).
11. Y. Feng, R. Mo, L. Wang, C. Zhou, P. Hong, and C. Li, "Surface enhanced Raman spectroscopy detection of sodium thiocyanate in milk based on the aggregation of Ag nanoparticles," Sensors 19(6),1363 (2019).
12. A. Nizamuddin, F. Arith, J. Rong, M. Zaimi, A. S. Rahimi, and S. Saat, "Investigation of copper (I) thiocyanate (CuSCN) as a hole transporting layer for perovskite solar cells application," Journal of Advanced Research in Fluid Mechanics and Thermal Sciences 78(2), 153–159 (2020).
13. Q. Tong, W. Wang, Y. Fan, and L. Dong, "Recent progressive preparations and applications of silver-based SERS substrates," TrAC Trends in Analytical Chemistry 106, 246–258 (2018).

14. Y. Zhang, R. J. Liu, X. Ma, X. Y. Liu, Y. X. Zhang, and J. Zhang, "Ag nanoparticle decorated MnO 2 flakes as flexible SERS substrates for rhodamine 6G detection," RSC Advances 8(66), 37750–37756 (2018).
15. T. Jiang, L. Zhang, H. Jin, X. Wang, and J. Zhou, "In situ controlled sputtering deposition of gold nanoparticles on MnO2 nanorods as surface-enhanced Raman scattering substrates for molecular detection," Dalton Transactions 44(16), 7606–7612 (2015).
16. L. Wu, Z. Wang, S. Zong, and Y. Cui, "Rapid and reproducible analysis of thiocyanate in real human serum and saliva using a droplet SERS-microfluidic chip," Biosensors and Bioelectronics 62, 13–18 (2014).
17. A. Hussain, H. Pu, and D. W. Sun, "SERS detection of sodium thiocyanate and benzoic acid preservatives in liquid milk using cysteamine functionalized core-shelled nanoparticles," Spectrochimica Acta Part A: Molecular and Biomolecular Spectroscopy 229, 117994 (2020).
18. Z. Wang, C. Ma, Y. Wu, J. Gu, C. Zhu, L. Li, and G. Chen, "A sensitive method for detecting sodium thiocyanate using AgNPs and MIL-101 (Fe) combined as SERS substrate," Vibrational Spectroscopy 117, 103311 (2021).
19. F. PulliShery, G. S. Panchmal, and S. SiDDique, "Salivary thiocyanate, uric acid and pH as biomarkers of periodontal disease in tobacco users and non-users-an in-vitro study," Journal of Clinical and Diagnostic Research 9(7), ZC47–ZC50 (2015).
20. Z. Ma, Y. Zhai, Z. Chen, H. Yang, and F. Wang, "Preparation of QSS@ AuNPs and Solvent Inducing Enhancement Strategy for Raman Determination of Salivary Thiocyanate," ACS Applied Materials & Interfaces 13(5), 5966–5974 (2021).
21. M. P. Noland, R. J. Kryscio, R. S. Riggs, L. H. Linville, L. J. Perritt, and T. C. Tucker, "Saliva cotinine and thiocyanate: Chemical indicators of smokeless tobacco and cigarette use in adolecents," Journal of Behavioral Medicine 11, 423–433 (1988).
22. I. M. Colceriu-Șimon, M. Hedeșiu, V. Toma, G. Armencea, A. Moldovan, G. Știufiuc, B. Culic, V. Țărmure, C. Dinu, I. Berindan-Neagoe, and R. I. Știufiuc, "The effects of low-dose irradiation on human saliva: A surface-enhanced raman spectroscopy study," Diagnostics 9(3), 101 (2019).